Cellular Decomposition in a Cu-25Ni-15Co Side-Band Alloy

MASAMICHI MIKI and DAVID E. LAUGHLIN

The process of decomposition in a Cu-25 mass pct Ni-15 mass pct Co alloy has been investigated by X-ray diffraction, optical and electron microscopy, and hardness measurements. The alloy first decomposed *via* spinodal decomposition, followed by a set of complex cellular-like reactions. X-ray diffraction results showed that side bands exist even after the spinodal microstructure has been completely replaced by the cellular-like microstructure. TEM showed that the cellular-like microstructure had a fiber-like appearance with high degree of periodicity. It is this structure which gives rise to the side bands in the X-ray diffraction pattern late in the transformation process. The primary cells engulfed the entire matrix after a short time of aging and were followed by secondary and tertiary cells. During these later reactions the fiber spacing increased and the composition of the phases reached their equilibrium values. This cellular-like transformation is different from the conventional cellular precipitation, and is interpreted as the preferential growth of part of the spinodal microstructure which is near the grain boundary, due to grain boundary migration. We call this type of cellular transformation in the spinodal alloys "cellular decomposition".

I. INTRODUCTION

THE cellular transformation conventionally has been defined as the transformation in which cells with a lamellar mixture of the *a* phase and the precipitate phase of equilibrium composition nucleate at grain boundaries and grow concomitantly into the matrix.[1] However, Miki and Amano recently reported a different type of cellular transformation in Cu-Ni rich Cu-Ni-Al side-band alloys.[2,3] In these alloys, neither the *a* nor the precipitate phase in the cells had the equilibrium compositions during the early stage of cell growth. Their composition changed gradually to the equilibrium values with the progress of aging. Moreover, the microstructure in cells was not pearlitic but consisted of a very fine set of fibers. The fibers formed an aligned periodic structure, but distinct X-ray side bands were not detected from these cells.

In order to ascertain if a periodic structure exists in the cells of these alloys and to elucidate the structure of these cells, the present work was performed on Cu-Ni-Co[4-9] and Cu-Ni-Fe[10-17] alloys, which are known to be typical side-band alloys. We will show the similar results on Cu-Ni-Fe alloy in a later paper.

Several papers[7,8,9] have been published on the age-hardening or intragranular transformation in Cu-Ni-Co alloys, but a detailed study by TEM and X-ray on the cellular transformation in these alloys has not been reported. Moreover, how the intragranular transformation in these alloys relates to the spinodal microstructure has not been clarified yet, though the X-ray side bands have been observed in the aged specimens. Therefore, this point was also investigated in the present work.

II. EXPERIMENTAL PROCEDURES

The chemical compositions of the alloy used in this work are presented in Table I. The section of Cu-Ni-Co phase diagram at 25 mass pct Ni is shown in Figure 1.[4] The composition of the alloy used in this work and its solution treatment and aging temperatures are denoted in this figure. The aging temperature is about 150 K below the estimated mean field spinodal. The alloy was prepared by melting Cu (99.9 pct), Ni (99.95 pct), and Co (99.5 pct) in a high purity alumina crucible in an Ar atmosphere. The ingot was

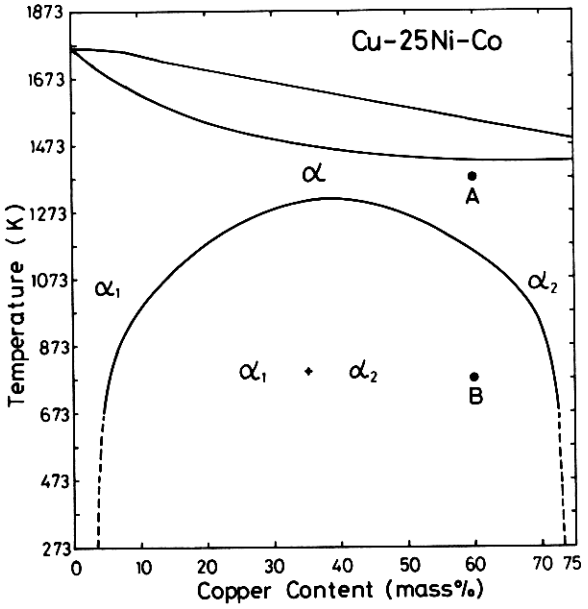

Fig. 1 — Vertical section of the Cu-Ni-Co phase diagram for a constant Ni content of 25 mass pct (Ref. 4). The solution treatment and aging temperatures of the alloy used in this work are denoted by the dots A and B, respectively.

Table I. Chemical Compositions of Alloy (Mass Pct)

Nominal	Cu	Ni	Co	Fe	Al, Ti, Si, Pb
Cu-25Ni-15Co	bal.	24.41	15.72	0.016	trace

MASAMICHI MIKI, Lecturer, Department of Materials Science, Himeji Institute of Technology, Himeji, Japan, is now Visiting Researcher, Department of Metallurgical Engineering and Materials Science, Carnegie-Mellon University, Pittsburgh, PA 15213. DAVID E. LAUGHLIN is Professor, Department of Metallurgical Engineering and Materials Science, Carnegie-Mellon University, Pittsburgh, PA 15213.

Manuscript submitted December 28, 1984.

homogenized at 1373 K and then cut into disks. The disks were then cold rolled and prepared for transmission electron microscopy (TEM), optical microscopy, hardness, and X-ray diffraction measurements. The specimens were again homogenized at 1373 K and quenched into iced brine, aged isothermally at 773 K, and then examined.

The hardness measurements were performed with a Vickers micro-hardness tester using a load of 2.94 N. Specimens for optical observation were etched by a $FeCl_3/HCl$ solution with 1:3 composition by volume. Thin foils for TEM observation were prepared by a twin-jet method in a HNO_3/CH_3OH solution with 1:2 composition by volume at −30 °C (243 K). The TEM observation was done by using JEM-100CX with a double tilting stage. The X-ray side bands were detected by using an X-ray diffractometer with a Cu target and a graphite monocrometer with a goniometer speed of $2\theta = 1/16°$ per minute (0.00011° per second).

III. RESULTS

A. *Optical Microscopic Observation*

The optical microstructures of specimens aged at 773 K after quenching from 1373 K are shown in Figure 2. In this alloy, growth of the cells took place after a very short aging time; *i.e.*, about 40 area pct of the matrix was engulfed by cells after only 30 s aging at 773 K (Figure 2(b)). As seen in Figure 2(b), the growth rates of cells were different at different grain boundaries; *e.g.*, the rate at the grain boundary A is slow but the rate at the grain boundary B is fast. Also, it can be seen that secondary cells already replaced the primary cells in some regions. See, for example, grain boundary B where the secondary cell (C2) has already replaced part of the primary cell (C1). After 300 seconds aging (Figure 2(c)), the primary cells engulfed the entire specimen, and the secondary cells became more visible (see, *e.g.*, cell (C2) in Figure 2(c)). After 3×10^4 s aging (Figure

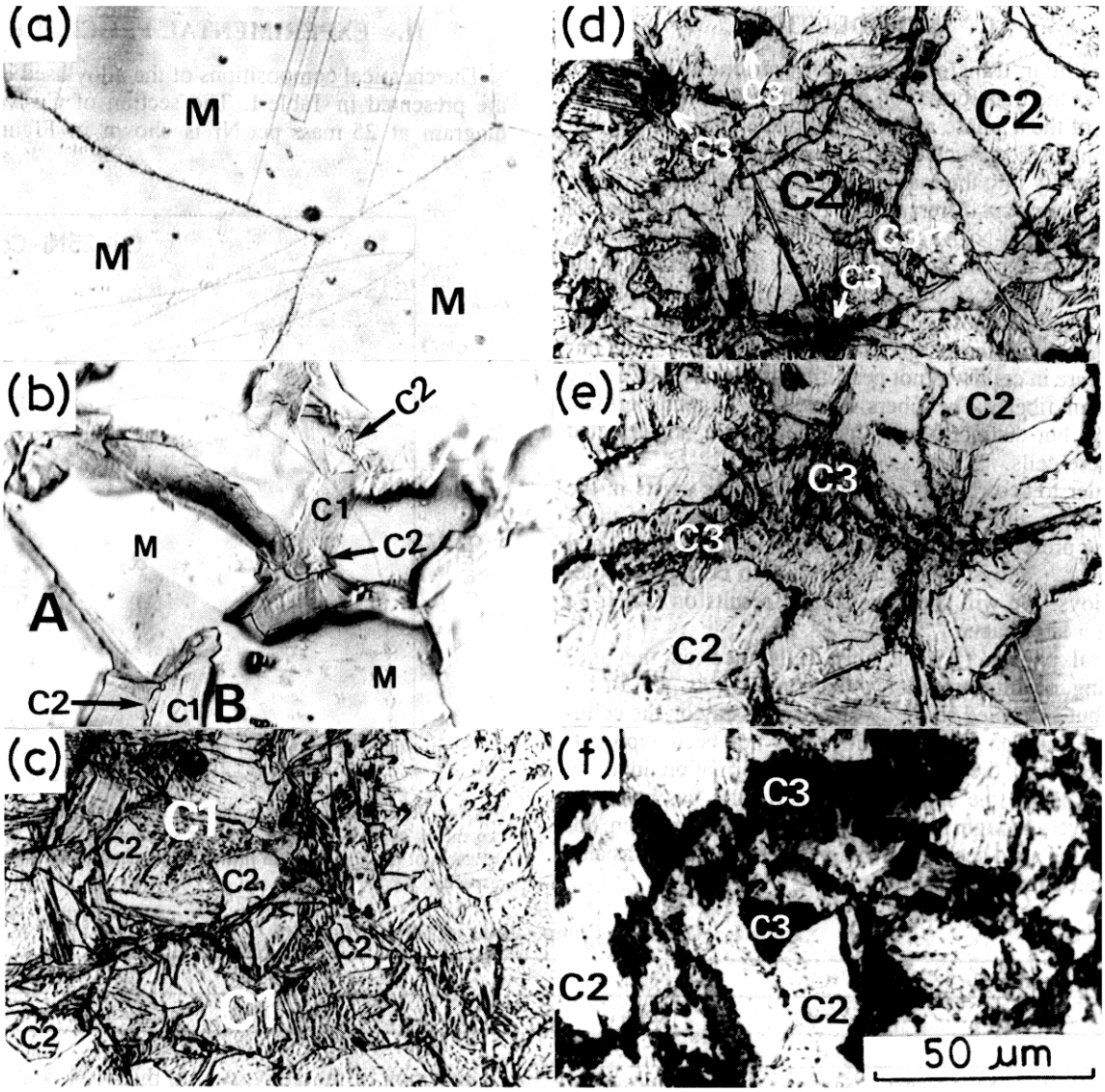

Fig. 2—Optical microstructures of specimens aged at 773 K after quenching from 1373 K. (*a*) As-quenched, (*b*) aged for 30 s, (*c*) aged for 300 s, (*d*) aged for 3×10^4 s, (*e*) aged for 6×10^4 s, and (*f*) aged for 10^6 s.

2(d)), the secondary cells completely engulfed the entire specimen and the formation of tertiary cells (C3) with very coarse precipitates were observed at the original and the advancing boundaries. With the progress of aging, these tertiary cells grew larger (Figures 2(e) and 2(f)). In all cases the microstructure in the cells could not be delineated clearly by optical microscopy.

B. *Hardness Change*

In Figure 3, the change in hardness during aging at 773 K is presented. The hardness of the matrix increased gradually with increasing time. The mean hardness of the cells showed a higher value than that of the matrix at the early stage of aging. It then increased further until the completion of the secondary cellular reaction. After the completion of the secondary cellular reaction, the mean hardness of the cell decreased with the increasing amount of the tertiary cells. The change in hardness of cells during aging suggests that both structural and compositional changes occur.

C. *X-Ray Diffraction Results*

The change in the X-ray diffraction pattern during the early stages of aging is displayed in Figure 4. Distinct X-ray side bands were observed in the specimen aged for 30 seconds at 773 K, although they were not observed in the as-quenched specimen. With the progress of aging, their intensity increased and their positions approached the main diffraction lines. These changes in the side bands after 300 seconds of aging are due to the growing amount of secondary and tertiary cells in the microstructure, since the primary cells had already completely engulfed the matrix after 300 seconds of aging (Figure 2(c)). The continued increase in the intensity of side bands after the completion of the primary cellular reaction demonstrates that the difference in composition between the two phases in the cells is increasing. The approach of the side bands to the main diffraction line shows that the two phase mixture is getting coarser with time.

The changes in the X-ray diffraction patterns during the later stages of aging are shown in Figure 5. After the completion of the secondary cellular reaction (3×10^5 s), new diffraction lines of the a_1 and a_2 phases were observed. Their peak heights increased and the positions of these peaks shifted slightly with the progress of aging. Thus the equilibrium composition of the two phases occurs after the tertiary cellular reaction is completed.

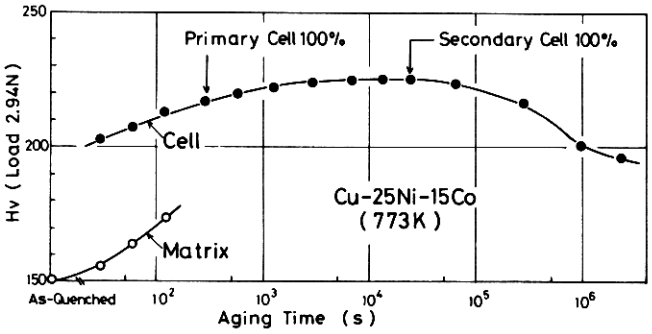

Fig. 3—Hardness *vs* time of the matrix and the cell in the Cu-25 mass pct Ni-15mass pct Co alloy on aging at 773 K.

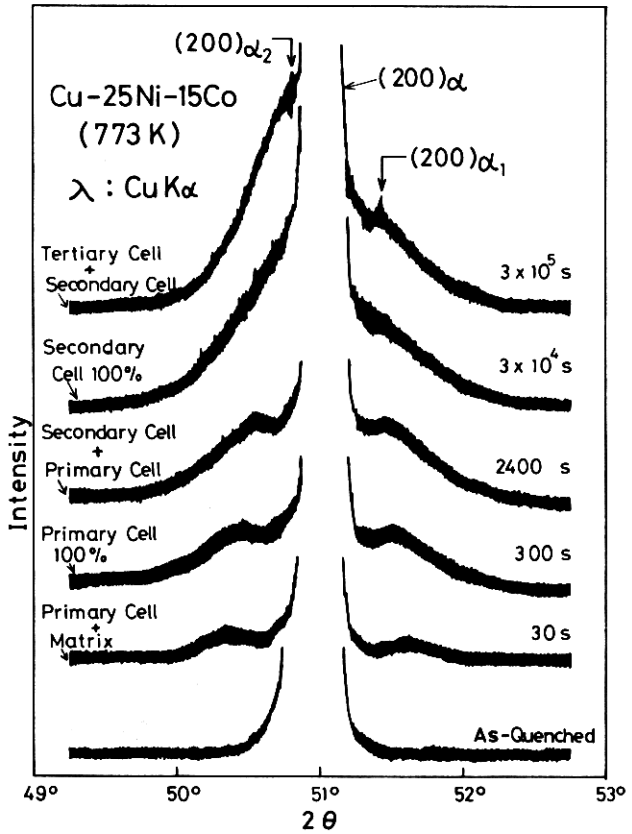

Fig. 4—Change in diffraction pattern of the Cu-25 mass pct Ni-15 mass pct Co alloy on aging at 773 K after quenching from 1373 K. Distinct side bands can still be observed after the completion of the primary cellular reaction, 300 s.

In Figure 6, the change in lattice parameter of the a phase in the cells on aging at 773 K is displayed. The lattice parameter in the cells changed only slightly until the completion of the secondary cellular reaction, after which the a phase separated into the a_1 and the a_2 phases. The lattice parameters of these phases changed to their equilibrium values with further aging. It is considered from the difference in these lattice parameters that the a_1 phase is rich in Co and the a_2 phase is rich in Cu, since the Co atoms are smaller than the Cu atoms.

D. *TEM Observation*

The microstructure of the matrix in the as-quenched specimen is shown in Figure 7. Modulation in contrast along the [100] direction is observed in this figure, and diffuse [100] satellites are observed around the $(\bar{2}00)$ reflection of the electron diffraction pattern from this area. These facts suggest that spinodal decomposition took place in the matrix during the continuous cooling from the spinodal temperature[18] during the quench. The wave length of the modulated structure calculated from the $(\bar{2}00)$ electron diffraction satellites is about 5 nm, agreeing well with that from the TEM contrast. The side bands due to this spinodal decomposition were not observed by X-ray diffraction in the as-quenched specimen as shown in Figure 4, although satellites were observed clearly in the TEM diffraction pattern of the as-quenched specimen as shown in this figure. This is because

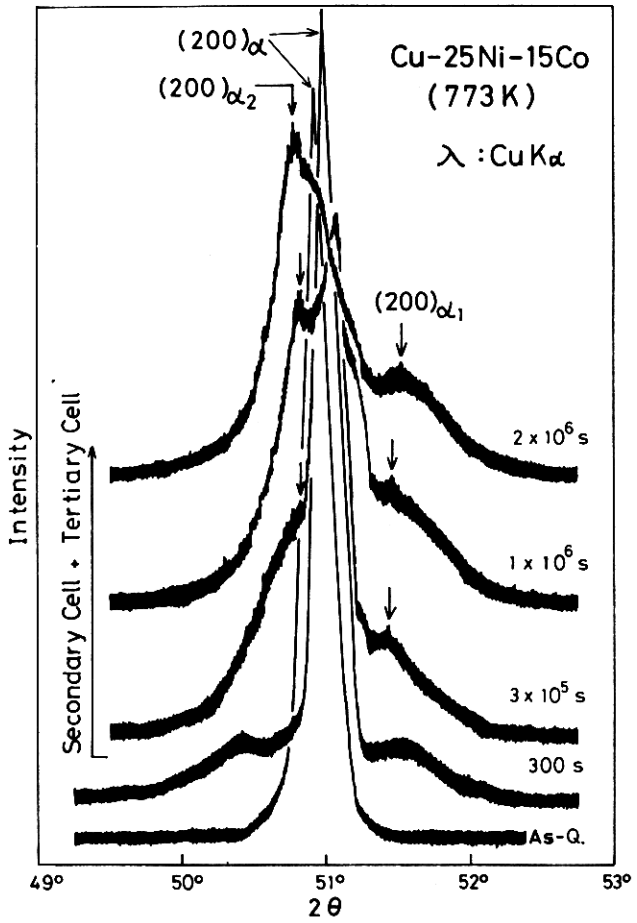

Fig. 5 — Change in diffraction pattern of the Cu-25mass pct Ni-15 mass pct Co alloy in the later stage of aging at 773 K.

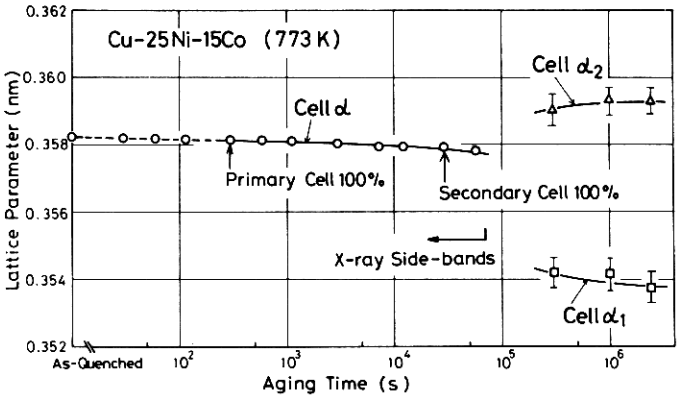

Fig. 6 — Change in lattice parameter of the *a* phase in the cell of the Cu-25 mass pct Ni-15 mass pct Co alloy on aging at 773 K.

the atomic scattering factor difference is larger for electrons than for X-rays in this alloy.

In Figure 8, the microstructure of the matrix in the specimen aged for 30 seconds at 773 K is shown. The TEM contrast and the shape of the diffraction satellites are almost the same as those of the as-quenched specimen. However, the wave length of the modulated structure appears to have increased slightly in comparison with that of the as-quenched specimen.

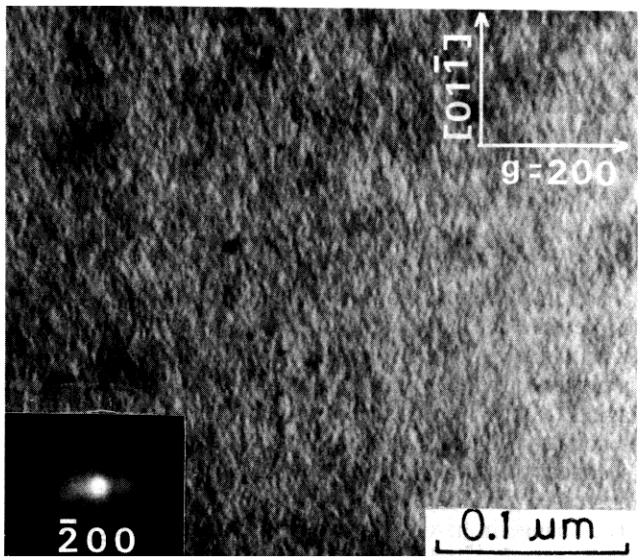

Fig. 7 — TEM microstructure and ($\bar{2}00$) reflection with corresponding satellites for the matrix of the Cu-25 mass pct Ni-15 mass pct Co alloy quenched from 1373 K. Electron beam is nearly perpendicular to (011) plane in the matrix.

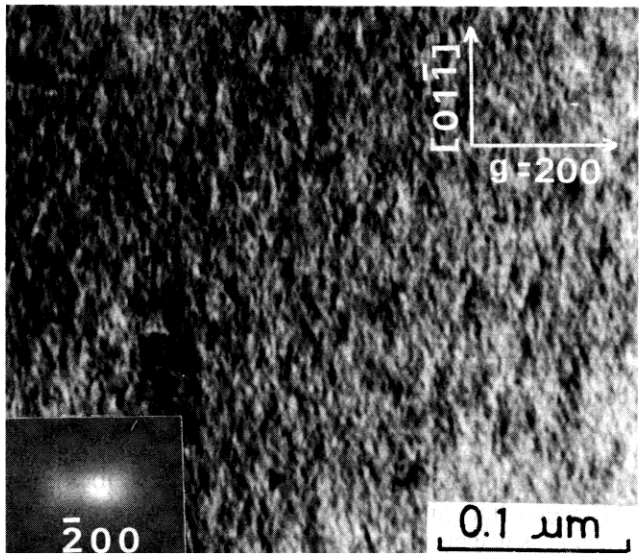

Fig. 8 — TEM microstructure and ($\bar{2}00$) reflection with corresponding satellites for the matrix of the Cu-25 mass pct Ni-15 mass pct Co alloy aged at 773 K for 30 s. Electron beam is nearly perpendicular to (011) plane in the matrix.

A typical microstructure inside the primary cell of the specimen aged for 30 seconds at 773 K is shown in Figure 9. A wavy fiber-like periodic structure is observed in this figure. The width (fiber-spacing) of the fiber-like structure is less than 10 nm. The direction of this wavy fiber-like structure appears to change continuously at places denoted by A, B, C, and D.

Figure 10 is a higher magnification photograph of a similar region. It shows more detail of the structure around the places where the fibers bend in the primary cells. Figure 10(a) is the bright-field image and Figure 10(b) is the diffraction pattern from this area. In Figure 10(c) the detail

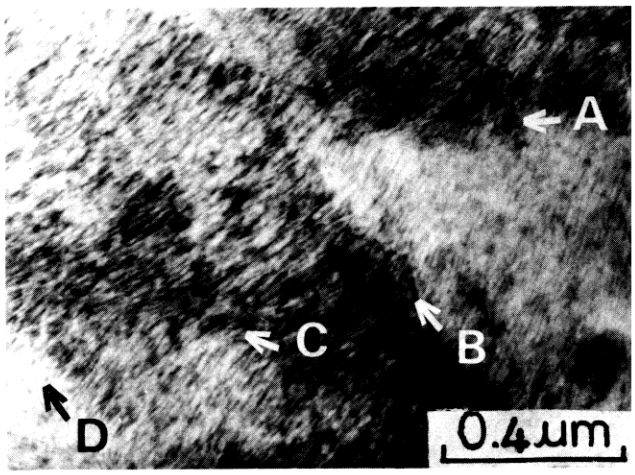

Fig. 9—TEM microstructure of the primary cell of the Cu-25 mass pct Ni-15 mass pct Co alloy aged at 773 K for 30 s.

of the $(\bar{1}1\bar{1})$ reflection can be observed. As seen from Figure 10(a), the direction of the fiber-like structures changes at the place denoted by C. As shown in Figures 10(b) and (c), two sets of satellites flank around each main reflection. The directions of two sets of satellites are perpendicular to the fiber-like structures in the two regions, A and B in Figure 10(a), but the positions of the main reflections from these regions coincide perfectly with each other. This means that the crystallographic orientations of the phases of the regions, A and B, are the same, although the directions of the fiber-like structure in two regions are different. Thus, C is not to be considered as a grain boundary. This phenomenon cannot be explained as pearlite-like lamellae with the arrangements of the phases along fixed habit planes of the matrix. The wave length (fiber spacing) of this fiber-like periodic structure is about 7 nm, nearly the same as that of the modulated structure in the matrix of the specimen aged at 773 K for 30 seconds, as shown in Figure 8.

In Figure 11, an example of the periodic structure in the secondary cells is shown. As seen from this figure, the wave length (the fiber spacing) of periodic structure, 10 to 13 nm, is larger than that in the primary cells shown in Figure 10. Moreover, distinct satellites also are observed around the main reflection in the diffraction pattern of the cell B. Hence, the side bands observed in the X-ray patterns (Figures 4 and 5) arise from the periodic fiber-like microstructure in the cellular region, and not from a microstructure due to spinodal decomposition.

The microstructure in the tertiary cells in the specimen aged for a long time, 6×10^4 seconds, at 773 K is shown in Figure 12. Coarse precipitates (arrow marks) are observed in the matrix of the tertiary cells, as shown in Figure 12(a). Some of them appear white because they have fallen out of the specimen during thinning. Comparing the volume fraction of these precipitates to the phase diagram in Figure 1, they are considered to be a_1 phase and the matrix

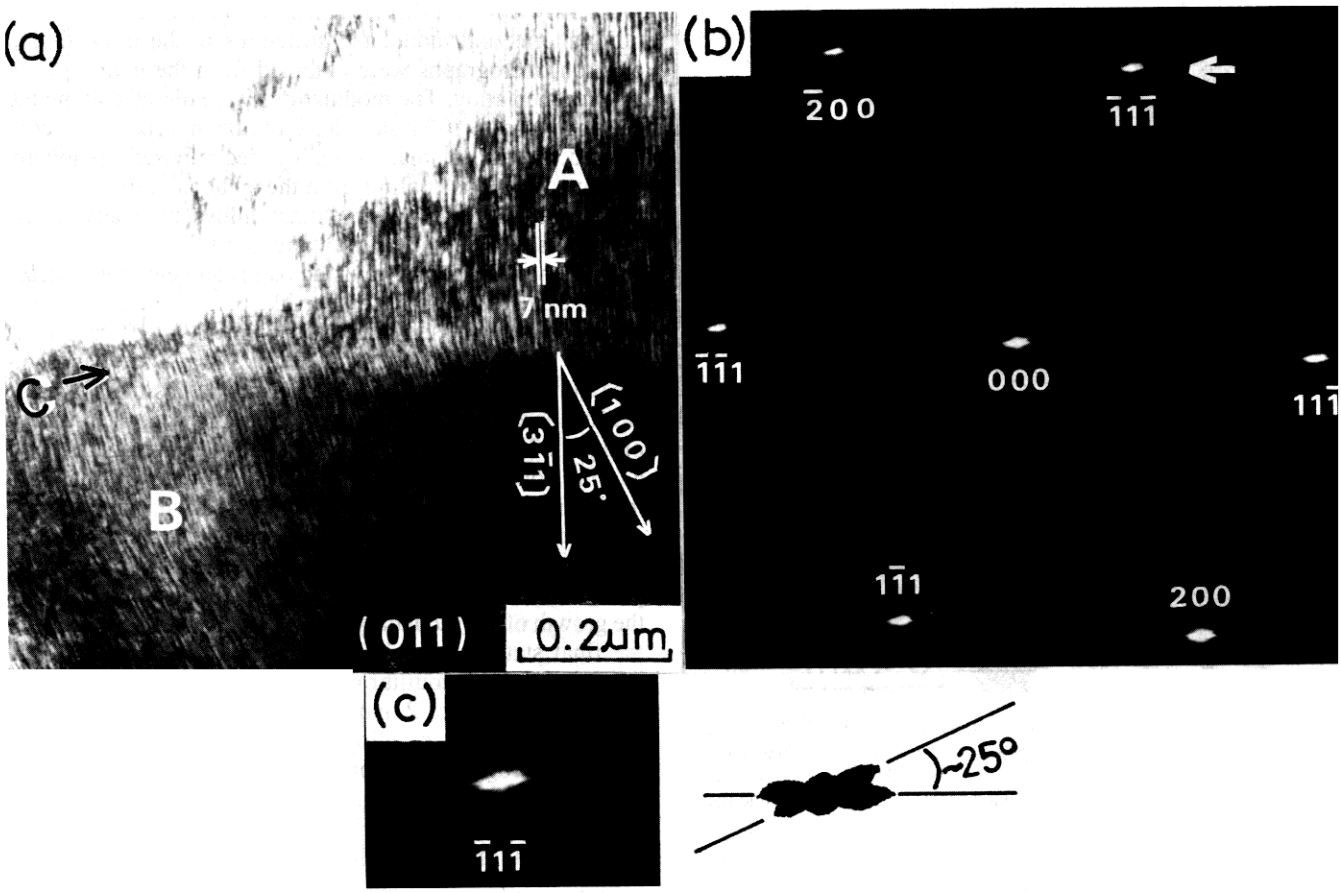

Fig. 10—TEM observations in the primary cell of the Cu-25 mass pct Ni-15 mass pct Co alloy aged at 773 K for 30 s. (*a*) Bright-field image, (*b*) the diffraction pattern of (a), and (*c*) enlarged photograph of $(\bar{1}1\bar{1})$ reflection in (b). Electron beam is perpendicular to (011) plane in the cell matrix phase.

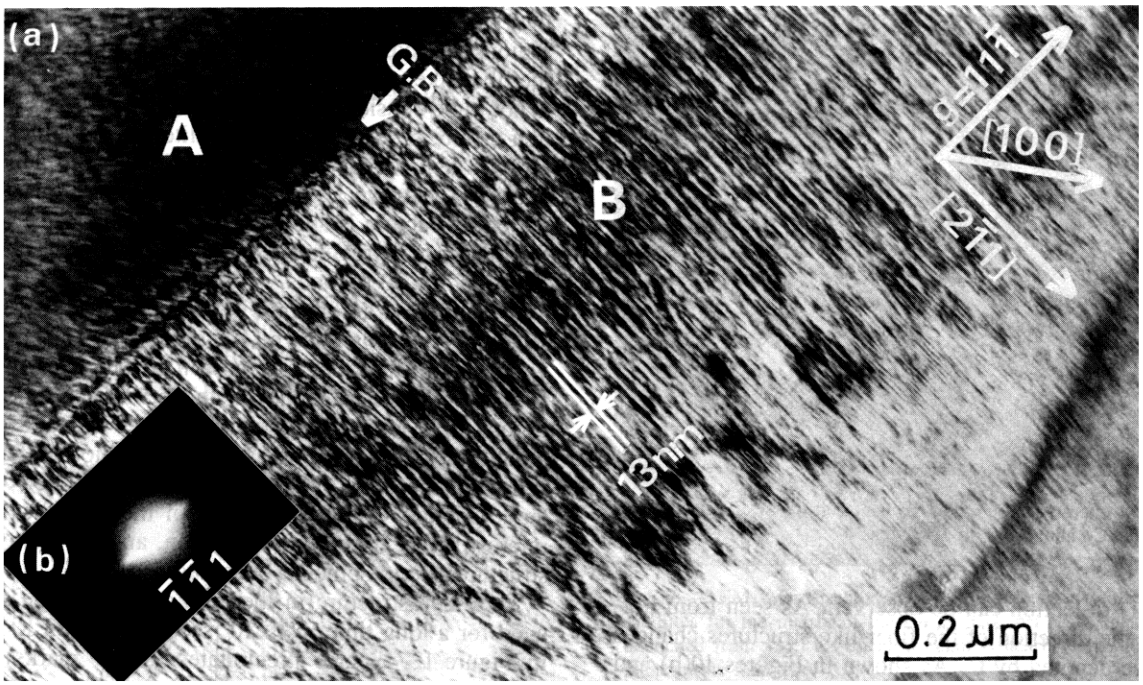

Fig. 11—TEM observation in the secondary cell of the Cu-25 mass pct Ni-15 mass pct Co alloy aged at 773 K for 30 s. (*a*) Bright-field image and (*b*) the $(\bar{1}\bar{1}1)$ reflection from diffraction pattern obtained from cell B. Electron beam is nearly perpendicular to the (011) plane in the cell B.

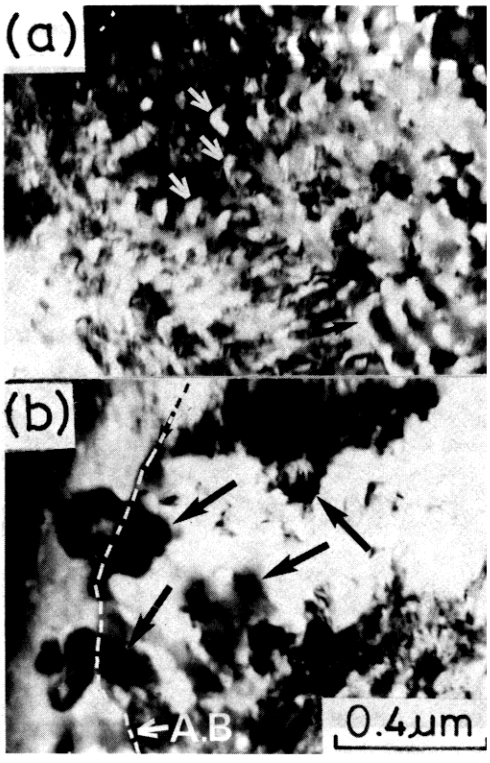

Fig. 12—TEM microstructures in the tertiary cells aged at 773 K for a long time, 6×10^4 s. Coarse precipitates denoted by arrow marks (a_1 phases) can be seen in the cell matrix (a_2 phase). (*a*) The precipitates in the central region of the tertiary cell and (*b*) the coarser precipitates around the advancing boundary (A.B).

to be the a_2 phase. Coarser precipitates (arrow marks) are observed near the advancing boundary, as shown in Figure 12(b). These a_1 and a_2 phases have nearly the equilibrium compositions.

IV. DISCUSSION

As shown above, diffuse satellites in the electron diffraction patterns and modulated structures in the transmission electron micrographs were obtained from the matrix of the as-quenched alloy. The modulations were directed along the elastically soft ⟨100⟩ directions of the matrix. It is considered, therefore, that this alloy decomposed spinodally during continuous cooling from the spinodal temperature as has been observed in many other alloys by many investigators (see Reference 19 for a review).

Moreover, distinct X-ray side bands and electron diffraction satellites as well as the fiber-like periodic structure were observed from the cells of the specimens aged for a short time at 773 K. The intensity of the X-ray side bands increased with increasing aging time and the positions of these side bands approached the main reflections with the progress of aging. These facts demonstrate that the average spacing and the composition difference between the two phases in the fiber-like periodic structure increased with the progress of aging. It is considered that the change in average spacing and composition difference between two phases in the periodic structure in the cell was mainly brought about by the growth of the secondary and the tertiary cells. Therefore, the final state is brought about by the full growth of the tertiary cells with equilibrium a_1 and equilibrium a_2 phases, as shown in Figures 2 and 6.

Other examples of alloys in which the cellular transformation progressed in three stages, as in this alloy, have been reported, *e.g.*, the Ni-Sn alloy.[20] However, in that alloy, one phase (the precipitate phase) in the cell already had the equilibrium composition from the primary cell formation and only the matrix phase in the cells changed its composition to the equilibrium value with the progress of aging. In the present alloy, both phases in the cell initially did not have the equilibrium compositions in the primary

cell formation stage. They changed their compositions gradually to the equilibrium values with the progress of aging. Moreover, these two phases in the cell showed the fiber-like periodic array in the early stage of aging. The wave length (fiber spacing) of this periodic structure in the primary cell was nearly the same as that of the modulated structure in the matrix. The growth direction of the fiber-like periodic structure changed flexibly while retaining the same crystallographic orientation of the phases, as shown in Figures 9 and 10. Thus, the characteristics of the cellular transformation in this alloy are different from those of the conventional cellular transformation. It is considered, from above facts, that the formation and growth mechanisms of the cell in this alloy are different from those of the conventional pearlitic cell.

The formation of the fiber-like periodic structure in the primary cell may be ascribed to the preferential growth of part of the spinodal structure in the matrix near the grain boundary due to grain boundary migration. As for the initiation of the grain boundary migration, a mechanism reported by Tanner[21] is helpful. He reported that initiation sites existing at high angle grain boundaries during the quench could rapidly grow into an adjacent grain, giving rise to a fiber-like microstructure. His model originally was applied to the single phase ordering reaction of a Ni_2V alloy, where the fibers were different domains of the ordered structure. The Cu-25 pct Ni-15 pct Co alloy decomposes spinodally during the quench. If the solute-enriched regions exist right up to the grain boundary during the quench, these regions may act as the initiation sites of the primary cell growth as the result of the accelerated decomposition. In the ordered Ni_2V alloy, the driving force for the cell growth was the difference in coherency strain energy between the cell and the matrix. However, in the Cu-25 pct Ni-15 pct Co alloy, the driving force for the primary cell growth is considered to be the difference in chemical free energy between the primary cell and the matrix, because the two phases in the cells are coherent with each other until the completion of the secondary cellular reaction. Thus, the cellular transformation in the Cu-25 pct Ni-15 pct Co alloy is interpreted as the preferential growth of part of the spinodal microstructure near a boundary by the migration of the boundary. This transformation is to be distinguished from the conventional "cellular precipitation". We call this type of transformation in spinodal alloys "cellular decomposition". Further work is planned to investigate the validity of the above-mentioned model to the cellular decomposition in the spinodal alloys.

V. SUMMARY

The characteristics of the cellular transformation in the Cu-25 pct Ni-15 pct Co side band alloy on aging at 773 K after quenching from 1373 K were investigated by X-ray diffraction analysis, optical and TEM observation, and hardness measurements. The results obtained are as follows:

1. Electron diffraction satellites and a modulated structure were observed from the matrix of the as-quenched specimens, indicating that this alloy decomposed spinodally during the quench from the solution-treatment temperature.
2. A second transformation (cellular type) occurred after the spinodal decomposition. The primary cells of this transformation engulfed the matrix entirely after only 300 seconds aging at 773 K, followed by the secondary cells. Distinct X-ray side bands, electron diffraction satellites, and the fiber-like periodic structures were obtained from both primary and secondary cells. The mean fiber spacing and the mean composition difference between two phases in the periodic structure in the cells increased with the growth of the secondary cells with coarser fiber spacing and larger composition difference than those of the primary cells.
3. The equilibrium state in the alloy was attained by the growth of tertiary cells with the equilibrium compositions of a_1 and a_2 phases.
4. The mean hardness of the cells increased with increasing aging time, and decreased with the growth of the tertiary cells.
5. It is considered that the formation and growth mechanisms of the cell in this alloy are different from those of the conventional cellular precipitation. A mechanism is discussed which relates the formation of the fiber-like periodic structure in the cells to the prior spinodal microstructure within the matrix. We call this type of cellular transformation in the spinodal alloys "cellular decomposition".

ACKNOWLEDGMENTS

The authors wish to thank Professor H. I. Aaronson, Professor T. Miyazaki (Nagoya Institute of Technology, Japan), and Mr. L. E. Tanner for helpful discussions. One of us (D. E. Laughlin) was partially supported by NSF Grant DMR-84-13115. Appreciation is also expressed to Professor Y. Ogino and to the Himeji Institute of Technology for granting a sabbatical leave to M. Miki.

REFERENCES

1. D. B. Williams and E. P. Butler: *International Metals Reviews*, 1981, vol. 26, no. 3, p. 153.
2. M. Miki and Y. Amano: *Trans. Japan Inst. Metals*, 1979, vol. 20, p. 1.
3. M. Miki and Y. Amano: *J. Japan Inst. Metals*, 1979, vol. 43, p. 551.
4. K. E. Volk, W. Dannöhl, and G. Masing: *Z. Metallkde.*, 1938, vol. 30, p. 113.
5. W. Dannöhl and H. Neumann: *Z. Metallkde.*, 1938, vol. 30, p. 217.
6. E. Biedermann and E. Kneller: *Z. Metallkde.*, 1956, vol. 47, p. 289.
7. A. H. Geisler and J. B. Newkirk: *Trans. AIME*, 1949, vol. 130, p. 101.
8. V. A. Phillips: *The Mechanism of Phase Transformations in Crystalline Solids*, Institute of Metals, London, 1968, p. 11.
9. S. Szymura, L. Sojka, and L. Skubela: *J. Mat. Sci.*, 1981, vol. 16, p. 3199.
10. V. Daniel and H. Lipson: *Proc. Roy. Soc.*, 1943, vol. A181, p. 368.
11. V. Daniel and H. Lipson: *Proc. Roy. Soc.*, 1944, vol. A182, p. 378.
12. V. Daniel: *Proc. Roy. Soc.*, 1948, vol. A192, p. 575.
13. E. P. Butler and G. Thomas: *Acta Metall.*, 1970, vol. 18, p. 347.
14. R. J. Livak and G. Thomas: *Acta Metall.*, 1971, vol. 19, p. 497.
15. R. J. Livak and G. Thomas: *Acta Metall.*, 1974, vol. 22, p. 589.
16. R. Gronsky and G. Thomas: *Acta Metall.*, 1975, vol. 23, p. 1163.
17. M. Hillert, M. Cohen, and B. L. Averbach: *Acta Metall.*, 1961, vol. 9, p. 536.
18. E. L. Huston, J. W. Cahn, and J. E. Hilliard: *Acta Metall.*, 1966, vol. 14, p. 1053.
19. W. A. Soffa and D. E. Laughlin: *Proceedings of An International Conference on Solid-Solid Phase Transformations*, H. I. Aaronson, D. E. Laughlin, R. F. Sekerka, and C. M. Wayman, eds., Met. Soc. AIME, 1982, p. 159.
20. M. Miki and Y. Ogino: *Trans. Japan Inst. Metals*, 1984, vol. 25, p. 603.
21. L. E. Tanner: *Acta Metall.*, 1972, vol. 20, p. 1197.